ELSEVIER

Journal of Nuclear Materials 298 (2001) 309–315

journal of nuclear materials

www.elsevier.com/locate/jnucmat

Activation of stainless steel with high energy neutrons

O. Grégoire, J. Ladrière *

Laboratoire de chimie inorganique et nucléaire, Université Catholique de Louvain (UCL), Chemin du Cyclotron 2, B-1348 Louvain-la-Neuve, Belgium

Received 20 July 2000; accepted 22 June 2001

Abstract

The development of the next generations of nuclear reactors (accelerator driven systems, ADS, or controlled fusion reactors) needs an important database of cross-sections for various nuclear reactions with high energy neutrons. At the cyclotron of Louvain-la-Neuve, a neutron beam has been developed on the base of a $^{9}Be(d,n)^{10}B$ reaction. The energy spectrum of the neutron beam is centered on 20 MeV. By using this tool, the activation of iron, chromium and nickel sheets has been measured, and the cross-section of various reactions has been calculated. Some of those cross-sections were available in the literature, and the comparison with our results shows the effect of delayed nucleon emission. The evaluation of the production rate of various isotopes, as well as the energy and relative intensity of their transitions, is very important to evaluate the activation of most stainless steels.

PACS: 28.41.Qb; 28.52.Fa; 29.25.Dz

1. Introduction

The next generations of nuclear reactors will use high energy neutrons. The energy of the neutrons emitted by a typical fusion reaction is 14 MeV, compared with a mean energy of 2 MeV for a fission reaction (furthermore, in most current reactors, the neutrons are thermalized in the core). Another project of future nuclear reactor concerns the accelerator driven systems (ADS). This kind of reactor, designed to produce electricity or to transmute long-lived radioactive waste, is based on a sub-critical fission core, coupled with a high current accelerator. This technology makes use of spallation neutrons produced on high-Z targets.

The use of high energy neutrons for the projects of the next generations of nuclear reactors (controlled fusion and ADS) needs new nuclear cross-section data to evaluate shielding requirements, activation and material damages. Most of the work performed in the field of material damages, for example, concerned irradiations with neutrons of a typical fission energy-spectrum. The effect of neutrons in this range of energy is well known, but the behaviour of high energy neutrons (in the range of 10th of MeV) is still under consideration. To address these needs, high flux neutron beams must be developed.

At the cyclotron of Louvain-la-Neuve, different fast neutron beams have been developed ($^{7}Li(p,n)^{7}Be$; $^{9}Be(p,n)^{9}B$; $^{9}Be(d,n)^{10}B$). The highest flux in the forward direction is obtained with the (d, n) reaction on a beryllium target [1]. We currently explore the possibilities of the use of this beam in the framework of damage analysis in stainless steel and, particularly, in austenitic stainless steels (Fe, Cr, Ni), selected as structural materials for the International Thermonuclear Experimental Reactor (ITER) [2,3].

Moreover, the activation of the reactor components represents a technical problem as well as the embrittlement. Therefore, it is important to determine the reactions induced by fast neutrons on the alloying elements of stainless steels. The irradiations enabled us to evaluate the activation of sheets of iron, chromium and nickel.

2. Irradiations

The stripping of deuterons on different targets enables the production of high neutron fluxes in the

* Corresponding author. Tel.: +32-10 473 102; fax: +32-10 473 115.

E-mail address: ladriere@chim.ucl.ac.be (J. Ladrière).

0022-3115/01/$ - see front matter
PII: S0022-3115(01)00647-X

forward direction. It has been shown [4] that the highest neutron flux with a (d, n) reaction is obtained with a thick beryllium target (10 mm in thickness).

Deuteron beams have been accelerated by the isochronous cyclotron of the University of Louvain. The accelerator delivers a 50 MeV deuteron beam with a maximum current of 10 μA. The intensity is measured by the current drawn from the electrically insulated production target made of beryllium. However, taking into account the rapid spatial variations in neutron flux that are expected, the integration of the deuteron beam intensity is not used to evaluate the neutron fluence. The on-line intensity measurement is only used to maintain the current as constant as possible. As we will see later, the neutron fluence is evaluated off-line according to activation measurements of witness iron sheets.

The beryllium block is water cooled to keep it at safe temperatures during the operation. The deuteron beam is focused as a 20 mm diameter spot on the target. A thick titanium collimator is used to protect the water-cooled copper piece surrounding the beryllium target against accidental deviation of the beam. A lead window is used to stop charged particles (Fig. 1).

The neutron energy spectrum has been obtained by unfolding the activity measurements of metallic foils with a code developed by Bernier et al. [1]. Its validity has been checked by comparison with previous measurements obtained by Meulders et al. [4] (Fig. 2).

The evaluation of the fluence reached during the irradiations was carried out with respect to the activity in ^{54}Mn of natural iron witness samples. These sheets are used as dosimeters through the reaction ^{54}Fe(n, p)^{54}Mn. This method has previously been used by Heinish et al. [5]. The neutron fluence f may be determined by the following expression:

$$f = \frac{\tau A \times 10^{24}}{N\sigma} e^{(t/\tau)} \ (\text{neutrons/cm}^2),$$

where τ is the lifetime of the ^{54}Mn nuclei (h), A is the activity of the samples (counts/h), t is the time elapsed since a reference time (the end of the irradiation), N is the amount of ^{54}Fe nuclei in the sample, and σ is the cross-section of the reaction (barns).

In order to avoid the use of the cross-section, a calibration of the activity of iron foils has been performed

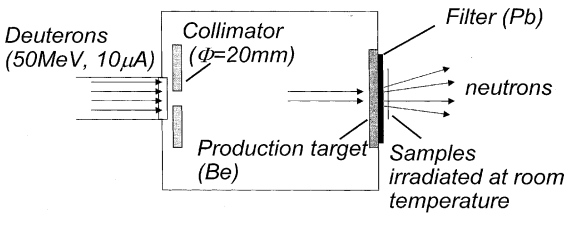

Fig. 1. Drawing of the neutron production device.

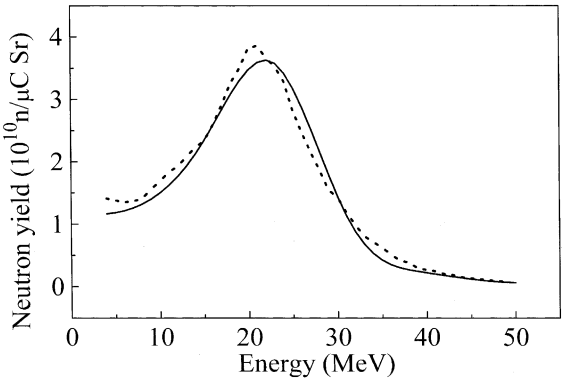

Fig. 2. Energy spectrum of neutrons obtained with 50 MeV deuterons on a thick beryllium target, deduced by unfolding [1] (solid line) and measured by Meulders et al. [4] (dotted line). These spectra correspond to the forward direction (less than 5°).

with samples irradiated at known fluences. The absolute neutron fluence is estimated from the activation of several metallic foils (In, Al, Co, Nb) through reactions of well-known cross-sections, covering the whole energy spectrum of neutrons. Production reactions and energy range of sensitivity of the induced radioactive nuclei are displayed in Table 1. The relative error of this technique is 20% [1].

To reach high fluences the samples are placed as close as possible to the production target, just after the filter of charged particles (Fig. 1). The samples (discs of 10 mm in diameter, 25 μm thick) stick on the outer face of the filter. This filter is made of 10 mm thick polystyrene plate intended for reduction of the proportion of low energy neutrons, followed by a 2 mm thick lead sheet. In these conditions the flux is close to 10^{12} neutrons/cm^2 s. Each treatment consists in a 10 h irradiation, allowing fluences of 2×10^{16} neutrons/cm^2 to be reached. The calculated fluence may vary from one irradiation to the other. However, in order to compare the results obtained after several irradiations, correction factors have been applied to account for the same fluence in each case. This is why all the results reported in

Table 1
Range of sensitivity of nuclear reactions used for the calibration of neutron fluence measurements

Reactions	Energy range (MeV)
^{115}In(n, γ)^{116m}In	Thermal
^{115}In(n, n′)^{115m}In	1–14
^{27}Al(n, α)^{24}Na	7–27
^{59}Co(n, γ)^{60}Co	Thermal
^{59}Co(n, p)^{59}Fe	4–30
^{59}Co(n, 2n)^{58}Co	14–50
^{59}Co(n, 3n)^{57}Co	>20
^{93}Nb(n, 2n)^{92m}Nb	9–30

this paper are related to a fluence of 2×10^{16} neutrons/cm^2. The duration of the irradiations is always the same.

3. Activity measurements

The tool used for gamma spectroscopy is a Ge–Li detector. The calibration of the scale of energy has been performed with different radioactive sources: ^{57}Co (122.1 and 136.4 keV), ^{22}Na (511.0 and 1274.5 keV), ^{137}Cs (661.6 keV), ^{54}Mn (834.8 keV) and ^{60}Co (1173.2 and 1332.5 keV).

The activity of a sample is the rate of disintegration, expressed in Becquerels. This value is different from the so-called specific activity ($A\gamma$), which is the rate of photon emission of a specific energy, and therefore depends on the relative intensity of the transition.

Taking into account the geometry and the efficiency of the counter with respect to the energy, the specific activity of the samples for each transition may be calculated

$$A\gamma = \frac{A_c}{T_c} F_G \frac{100}{\mathrm{Eff}} e^{(t/\tau)},$$

where A_c is the amount of counts (integrated) for the peak, T_c is the counting time, F_G is a factor of geometry, taking into account the distance between the sample and the detector, and the geometry of the sample. *Eff* is the efficiency of the counter depending on the gamma ray energy, t is the time elapsed since the end of the irradiation, and τ is the lifetime of the isotope.

Table 2
Activation of chromium, iron and nickel foils

Energy (keV)	Isotope	Half-life (d) [6]	Measured half-life (d)	$A\gamma$ (photons h^{-1} g^{-1})
Iron				
169	^{52}Fe	0.34	0.36 ± 0.05	1.56×10^8
320	^{51}Cr	27.72	27.85 ± 1.14	5.71×10^7
744	^{52}Mn	5.67	5.62 ± 1.16	4.51×10^8
835	^{54}Mn	312.5	321.2 ± 11.9	4.77×10^8
847	^{56}Mn	0.11		3.6×10^{11}
	^{56}Co	77.3		1.56×10^7
936	^{52}Mn	5.67	5.56 ± 0.19	5.13×10^8
1434	^{52}Mn	5.67	5.66 ± 0.07	5.41×10^8
Chromium				
159	^{47}Sc	3.4	3.39 ± 0.04	1.85×10^8
320	^{51}Cr	27.72	28.3 ± 0.3	2.64×10^9
744	^{52}Mn	5.67	5.66 ± 0.69	1.31×10^7
936	^{52}Mn	5.67	5.9 ± 0.5	1.27×10^7
984	^{48}Sc	1.83		5.13×10^8
	^{48}V	16.2		2.6×10^8
1038	^{48}Sc	1.83	1.82 ± 0.01	5.18×10^8
1312	^{48}Sc	1.83	1.91 ± 0.06	5.31×10^8
	^{48}V	16.2	16.36 ± 0.79	2.52×10^8
1434	^{52}Mn	5.67	5.88 ± 0.38	1.57×10^7
Nickel				
122	^{57}Co	272	305 ± 19	1.45×10^9
127	^{57}Ni	1.5		2.8×10^9
136	^{57}Co	272	289 ± 10	2.0×10^8
158	^{56}Ni	6.1	6.8 ± 0.8	8.22×10^7
270	^{56}Ni	6.1	6.5 ± 0.5	3.76×10^7
744	^{52}Mn	5.67	7.2 ± 1.1	3.67×10^7
811	^{58}Co	71.3	73.5 ± 2.1	7.8×10^9
835	^{54}Mn	312.5	362 ± 48	8.5×10^7
847	^{56}Mn	0.11		2.45×10^9
	^{56}Co	77.3	82.5 ± 2.7	6.31×10^8
931	^{55}Co	0.73	0.72 ± 0.09	5.37×10^8
1038	^{56}Co	77.3	80.4 ± 10.7	8.74×10^7
1238	^{56}Co	77.3	75.4 ± 1.8	4.4×10^8
1378	^{57}Ni	1.5	1.57 ± 0.02	2.84×10^{10}
1758	^{57}Ni	1.5	1.59 ± 0.04	2.19×10^9
1920	^{57}Ni	1.5	1.55 ± 0.02	5.11×10^9

The activity of the samples for each isotope is therefore

$$A_0 = A\gamma \frac{100}{I\gamma},$$

where $I\gamma$ is the intensity of the transition (%).

This activity may also be expressed by Bernier et al. [1]

$$A_0 = N\sigma\Phi(1 - e^{-t_{irr}/\tau}),$$

where σ is the cross-section of the activation reaction, N is the number of target nuclei in one gram of sample, t_{irr} is the duration of the irradiation (36 000 s) and Φ is the neutron flux (cm^{-2} s^{-1}). Therefore, if we replace Φ by the ratio of the fluence F (in neutrons/cm^2) on t_{irr}:

$$\sigma \text{ (barns)} = 10^{24} \frac{A_0 t_{irr}}{NF} \left(1 - e^{-t_{irr}/\tau}\right)^{-1}.$$

4. Results and discussions

The time-dependent spectral analysis of the activity of irradiated metals showed us the production of various isotopes in chromium, iron and nickel. The results are displayed in Table 2.

The specific activity (last column) is the total amount of photons emitted, taking into account the efficiency and the geometry of the detector, calculated at the end of an irradiation (2×10^{16} neutrons/cm^2 in 10 h). The possible production processes of those isotopes are summarized in Table 3.

In order to determine the cross-section of various reactions, the activity of each isotope has been calculated, taking into account the probability of each transition [6] (Table 4).

In Table 5, the second column represents the cross-sections available in the literature [7,8]. Those cross-sections are available below 20 MeV. The shape of the neutron spectrum in this range of energy has been taken into account. The third column displays the cross-sections calculated on the base of the activity of the products. The uncertainty of the measures is mainly due to the uncertainty in the evaluation of the neutron fluence, which has been estimated to nearly 20%. The efficiency of the germanium detector also counts for a few percent. Other sources of uncertainty (statistical errors during the countings, mass of the samples, literature related information such as lifetime of the isotopes or natural abundances) represent less than one percent. The total uncertainty of the results is in the range from 25% to 30%, varying with the energy of the gamma ray.

In some cases, the radioactive nucleus used for the determination of the cross-section may be produced directly by a nuclear reaction or indirectly, after the disintegration of another nucleus. Both reactions are then involved in the production of the isotope.

If we compare our results with the few data available in the literature, we see that the results are in good agreement for the reactions on ^{54}Fe. For the other reactions, our calculated value is lower than expected. However, we should keep in mind that in the literature, the cross-sections are only available below 20 MeV.

The results of our study suggest a sharp decrease of the cross-sections beyond 20 MeV. This has besides been suggested for the reaction $^{58}Ni(n, p)^{58}Co$ [9] but does not seem consistent with results obtained for the reaction $^{52}Cr(n, 2n)^{51}Cr$ [10].

It should also be noted that after a reaction with a high energy neutron, the nuclei are not in the ground state but are highly excited. If the excitation energy exceeds 7–12 MeV (neutron- or proton-separation energy [5]), the stabilisation of the nucleus may be achieved by

Table 3
Possible production processes of identified radioactive isotopes

Identified isotopes	Possible production processes	Disintegration products
^{47}Sc (β^-/3.4 d)	$^{50}Cr(n, n3p)^{47}Sc$	^{47}Ti stable
^{48}Sc (β^-/43.8 h)	$^{50}Cr(n, 3p)^{48}Sc$	^{48}Ti stable
^{48}V (EC, β^+/16.2 d)	$^{50}Cr(n, p2n)^{48}V$	^{48}Ti stable
^{51}Cr (EC/27.72 d)	$^{54}Fe(n, \alpha)^{51}Cr$	^{51}V stable
	$^{52}Cr(n, 2n)^{51}Cr$	
	$^{53}Cr(n, 3n)^{51}Cr$	
^{52}Mn (EC, β^+/5.67 d)	$^{54}Fe(n, p2n)^{52}Mn$	
^{54}Mn (EC/312.5 d)	$^{54}Fe(n, p)^{54}Mn$	^{54}Cr stable
^{56}Mn (β^-/2.64 h)	$^{56}Fe(n, p)^{56}Mn$	
^{52}Fe (β^+/8.3 h)	$^{54}Fe(n, 3n)^{52}Fe$	$^{52}Mn \rightarrow {}^{52}Cr$ stable
^{55}Co (β^+/17.5 h)	$^{58}Ni(n, p3n)^{55}Co$	$^{55}Fe \rightarrow {}^{55}Mn$ stable
^{56}Co (EC, β^+/77.3 d)	$^{58}Ni(n, p2n)^{56}Co$	^{56}Fe stable
^{57}Co (EC/272 d)	$^{58}Ni(n, pn)^{57}Co$	^{57}Fe stable
^{58}Co (EC, β^+/71.3 d)	$^{58}Ni(n, p)^{58}Co$	^{58}Fe stable
^{56}Ni (EC/6.1 d)	$^{58}Ni(n, 3n)^{56}Ni$	
^{57}Ni (EC, β^+/35.94 h)	$^{58}Ni(n, 2n)^{57}Ni$	$^{57}Co \rightarrow {}^{57}Fe$ stable

Table 4
Activity of the radioactive isotopes produced

Sample	Produced isotope	Activity (Bq/g)
Iron	^{51}Cr	1.60×10^5
	^{52}Mn	1.50×10^5
	^{54}Mn	1.33×10^5
	^{56}Mn	1.0×10^8
	^{52}Fe	3.89×10^4
Chromium	^{47}Sc	7.33×10^4
	^{48}Sc	1.47×10^5
	^{48}V	7.19×10^4
	^{51}Cr	7.42×10^6
Nickel	^{55}Co	2.04×10^5
	^{56}Co	1.79×10^5
	^{57}Co	4.44×10^5
	^{58}Co	2.17×10^6
	^{56}Ni	2.50×10^4
	^{57}Ni	8.89×10^6

the emission of a delayed particle (proton or neutron). For example, ^{56}Co may be produced by a (n, pn) reaction on ^{58}Ni, followed by the emission of a neutron. On the other hand, the production of ^{57}Ni may be followed by the emission of a neutron or a proton, leading to the formation of ^{56}Ni or ^{56}Co.

Hence, the cross-section of production of ^{57}Ni is lower than the cross-section of the reaction ^{58}Ni(n, 2n)^{57}Ni. The same phenomenon may be applied for most other reactions.

In this work, the calculated cross-section is the activation cross-section, corresponding to the production of radioactive isotopes. Those results may be easily used for the determination of the activation of steels, more easily than with the reaction cross-section data.

Some activation measurements have been performed on austenitic stainless steels of different types (AISI 304, 310, 316 and 316_{Ti}). Stainless steel 316_{Ti} has been provided by the Belgian centre for nuclear studies (CEN-SCK, Mol). Other grades have been purchased to

Table 5
Cross-sections of some nuclear reactions in the energy range of the neutrons spectrum

Nuclear reactions	Cross-sections [7,8] (mb)	Measured cross-sections (mb)
^{50}Cr(n, p2n)^{48}V		13.9 ± 3.5
^{50}Cr(n, 3p)^{48}Sc		3.5 ± 0.9
^{50}Cr(n, n3p)^{47}Sc		3.1 ± 0.8
^{52}Cr(n, 2n)^{51}Cr	275 ± 100	133 ± 33
^{54}Fe(n, 3n)^{52}Cr	50 ± 15	42.9 ± 10.7
^{54}Fe(n, 3n)^{52}Fe		8.4 ± 2.1
^{54}Fe(n, p2n)^{52}Mn		
^{54}Fe(n, 3n)^{52}Fe		0.21 ± 0.05
^{54}Fe(n, p)^{54}Mn	300 ± 100	398 ± 100
^{56}Fe(n, p)^{56}Mn	65 ± 20	19.6 ± 4.9
^{58}Ni(n, p3n)^{55}Co		0.16 ± 0.04
^{58}Ni(n, 3n)^{56}Ni		12.3 ± 3.1
^{58}Ni(n, p2n)^{56}Co		
^{58}Ni(n, 2n)^{57}Ni	540 ± 100	108 ± 27
^{58}Ni(n, pn)^{57}Co		
^{58}Ni(n, p)^{58}Co	300 ± 100	137 ± 34
^{58}Ni(n, 3n)^{56}Ni		0.14 ± 0.04
^{58}Ni(n, 2n)^{57}Ni	30 ± 10	13 ± 3

Table 6
Composition of the alloys[a]

Composition of the alloys (wt%)	AISI 304	AISI 310	AISI 316	AISI 316_{Ti}
Chromium	18 (17.7)	24 (21.8)	18 (15.9)	17 (16.5)
Nickel	10 (11.6)	20 (21.2)	10 (13.9)	11 (13.5)
Manganese	1 (1.7)	1 (1.7)	1 (0.9)	1 (0.8)
Molybdenum	–	–	3	2
Titanium	– (<0.01)	– (<0.04)	– (<0.02)	0.3 (0.27)
Carbon	<0.1	<0.25	<0.1	<0.1
Iron	Balance (65.1)	Balance (52.4)	Balance (64.5)	Balance (65.3)

[a] The first values are those commonly attributed to these types of alloys. The values in brackets have been measured by atomic absorption.

Table 7
Activation of different stainless steels (specific activity in photons h^{-1} g^{-1}) at the end of an irradiation of 2×10^{16}neutrons/cm^2 in 10 h

Energy (keV)	Isotope	AISI 304	AISI 310	AISI 316	AISI 316_{Ti}	18-10 SS
122	^{57}Co	1.6×10^8	2.4×10^8	1.8×10^8	1.3×10^8	1.45×10^8
127	^{57}Ni	4.28×10^8	6.36×10^8	4.57×10^8	3.22×10^8	2.8×10^8
136	^{57}Co	1.95×10^7	3.0×10^7	2.19×10^7	1.6×10^7	2.0×10^7
140	^{99}Tc	5.65×10^7		6.29×10^8	4.31×10^8	
159	^{47}Sc	2.97×10^7	3.5×10^7	3.06×10^7	6.49×10^7	3.3×10^7
	^{56}Ni	7.67×10^6	1.6×10^7	7.68×10^6	1.88×10^7	8.22×10^6
181	^{99}Mo			3.08×10^7	1.93×10^7	
320	^{51}Cr	4.87×10^8	4.37×10^8	3.82×10^8	3.09×10^8	5.15×10^8
744	^{52}Mn	3.23×10^8		3.39×10^8	3.0×10^8	3.22×10^8
778	^{99}Mo			1.8×10^7	4.3×10^7	
	^{96}Nb			2.6×10^8	1.2×10^8	
811	^{58}Co	6.8×10^8	1.2×10^9	7.8×10^8	6.4×10^8	7.8×10^8
835	^{54}Mn	3.74×10^8	2.37×10^8	2.99×10^8	2.69×10^8	3.42×10^8
847	^{56}Mn	2.5×10^{11}	1.5×10^{11}	2.2×10^{11}	1.8×10^{11}	2.52×10^{11}
	^{56}Co	7.5×10^7	1.1×10^8	8.62×10^7	6.5×10^7	7.4×10^7
936	^{52}Mn	3.84×10^8	2.6×10^8	3.54×10^8	2.9×10^8	3.61×10^8
984	^{48}Sc	8.38×10^7	8.5×10^7	4.8×10^7	1.59×10^8	9.23×10^7
	^{48}V	4.67×10^7	4.7×10^7	4.0×10^7	3.23×10^7	4.68×10^7
1038	^{48}Sc		1.2×10^8	8.0×10^7	1.6×10^8	9.32×10^7
	^{56}Co		1.2×10^7	9.5×10^6	7.66×10^6	8.74×10^6
1121	^{46}Sc				3.4×10^6	
1238	^{56}Co	4.4×10^7	7.0×10^7	5.28×10^7		4.4×10^7
1312	^{48}Sc	8.95×10^7	1.0×10^8	8.9×10^7	1.38×10^8	9.56×10^7
	^{48}V	4.43×10^7	4.3×10^7	3.3×10^7	2.73×10^7	4.54×10^7
1378	^{57}Ni	3.46×10^9	5.1×10^9	3.77×10^9	2.77×10^9	2.84×10^9
1434	^{52}Mn	3.97×10^8	2.31×10^8	3.09×10^8	3.04×10^8	3.82×10^8
1758	^{57}Ni	2.65×10^8	4.1×10^8	2.25×10^8	1.8×10^8	2.19×10^8
1920	^{57}Ni	6.26×10^8	8.2×10^8	7.11×10^8	4.67×10^8	5.11×10^8

The last column displays values of induced activity in a typical 18–10 stainless steel calculated on the base of activation results of iron, chromium and nickel foils (Table 2).

Goodfellow (Huntington, GB). The composition of those alloys is displayed in Table 6. The results obtained (Table 7) are in good agreement with the values foreseen on the base of the activity of iron, chromium and nickel. These values are reported in the last column for a typical AISI 304 composition (18% Cr, 10% Ni, 70% Fe). Moreover, the production of radioactive niobium and molybdenum isotopes has been shown in the steels containing molybdenum (AISI 316 and 316_{Ti}). In AISI 316_{Ti}, the production of ^{46}Sc and an increase of the production of ^{47}Sc and ^{48}Sc has also been shown, due to the presence of titanium.

5. Conclusions

Our study enables the evaluation of the production rate of radioactive nuclei in stainless steels irradiated with fast neutrons.

The activation cross-sections of some reactions have been evaluated in the energy range of 20 MeV. These cross-sections take into account the delayed emission of nucleons after nuclear reaction.

When the reaction cross-sections were available, the data were limited to neutron energies of 20 MeV. For these reactions, our results suggest a sharp decrease of the cross-section beyond 20 MeV, except for the reactions ^{54}Fe(n, α)^{51}Cr and ^{54}Fe(n, p)^{54}Mn.

Acknowledgements

The financial support has been supplied by the FRIA (fonds pour la Formation à la Recherche dans l'Industrie et l'Agriculture) and the IISN (Institut Interuniversitaire des Sciences Nucléaires). We would like to thank Jean Cara, Robert Dolhen and Pierre Nemegeer for their technical support. The cyclotron staff of Louvain-la-Neuve is also gratefully aknowledged for the efficient operation of the accelerator.

References

[1] K. Bernier, T. El Bardouni, Gh. Grégoire, O. Grégoire, Fast neutron irradiation facilities in Louvain-la-Neuve, Internal Report UCL-IPN-96-P02, 1996.

[2] N. Yoshida, J. Nucl. Mater. 205 (1993) 344.
[3] A.B. Korostelev et al., J. Nucl. Mater. B 237 (1996) 1361.
[4] J.P. Meulders et al., Nucl. Instrum. and Meth. 126 (1975) 81.
[5] H.L. Heinish et al., J. Nucl. Mater. 141–143 (1986) 807.
[6] Nuclear Data Group, Oak Ridge National Laboratory, Nuclear Level Schemes, $A = 45$ Through $A = 257$, Academic press, New York, 1973.
[7] V. Mc Lane et al., Neutron Cross Sections, vol. II, Academic Press, San Diego, CA, 1988.
[8] M.B. Chadwick et al., Nucl. Sci. Eng. 131 (1999) 293.
[9] M.J. Saltmarsh et al., Nucl. Instrum. and Meth. 145 (1977) 81.
[10] H. Liskien et al., Ann. Nucl. Energy 16 (11) (1989) 563.